Supplementary Information

RoboCap: Robotic mucus-clearing capsule for enhanced drug delivery in the gastrointestinal tract

Authors:
Shriya S. Srinivasan[1,2,3,†], Amro Alshareef[1,2,3], Alexandria V. Hwang[1,2,3], Ziliang Kang[1,2], Johannes Kuosmanen[3], Keiko Ishida[2,3], Joshua Jenkins[3], Sabrina Liu[3], Wiam Abdalla Mohammed Madani[2,3], Jochen Lennerz[4], Alison Hayward[2,3,5], Josh Morimoto[3], Nina Fitzgerald[3], Robert Langer[1,3], Giovanni Traverso[1,2,3,†]

[1]Department of Mechanical Engineering, Massachusetts Institute of Technology, Cambridge, MA 02139, USA.
[2]Division of Gastroenterology, Hepatology and Endoscopy, Brigham and Women's Hospital, Harvard Medical School, Boston, MA 02115, USA.
[3]David H. Koch Institute for Integrative Cancer Research, Massachusetts Institute of Technology, Cambridge, MA 02139, USA.
[4]Departnent of Pathology, Massachusetts General Hospital, Boston, MA 02114, USA.
[5]Division of Comparative Medicine, Massachusetts Institute of Technology, Cambridge, MA 02139, USA.
[†]Please address correspondence to: shriyas@mit.edu (S.S.S.), cgt20@mit.edu, ctraverso@bwh.harvard.edu (G.T.)

Supplementary Video 1: Mixing and wicking of viscous mucus (stained red) in luminal fluid (green) by the RoboCap and its recessed surface can be observed.

Supplementary Movie 2: Videography of this feature evinces significantly greater turbulence and mixing of viscous mucus (red) in luminal fluid (green).

Supplementary Movie 3: Simulation shows surface features wicking fluid during rotation.

Absorbance (O.D)	Time (min)	0	5	10	15	20	30
	50 Hz						
	Top	0.045	0.048	0.052	0.046	0.046	0.047
	Middle	0.044	0.055	0.051	0.053	0.048	0.046
	Bottom	0.047	0.062	0.065	0.063	0.056	0.048
	80 Hz						
	Top	0.0442	0.044	0.046	0.045	0.048	0.046
	Middle	0.0444	0.044	0.048	0.047	0.050	0.055
	Bottom	0.044	0.070	0.062	0.048	0.055	0.056
	120 Hz						
	Top	0.045	0.047	0.049	0.049	0.050	0.050
	Middle	0.0445	0.046	0.052	0.051	0.052	0.050
	Bottom	0.0447	0.161	0.067	0.058	0.051	0.048
	0 Hz						
	Top	0.049	0.045	0.044	0.044	0.048	0.045
	Middle	0.043	0.044	0.046	0.047	0.052	0.046
	Bottom	0.043	0.058	0.056	0.068	0.066	0.067

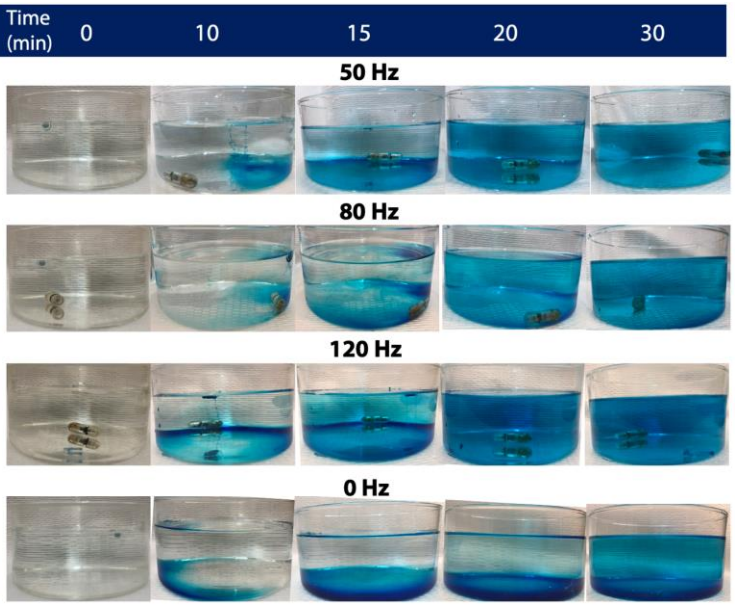

Supplementary Figure 1. Optical absorbance of samples from the top, middle, and bottom sections of the reaction chamber with drug (blue) and a RoboCap operating at frequencies of 0 (control), 50, 80, and 120 Hz. Faster dissolution is visualized by the high contrasted segments for the non-control chambers at 5 and 10 minutes. Even dispersion is achieved at 20 and 30 minutes for those chambers employing an RoboCap as compared to the control.

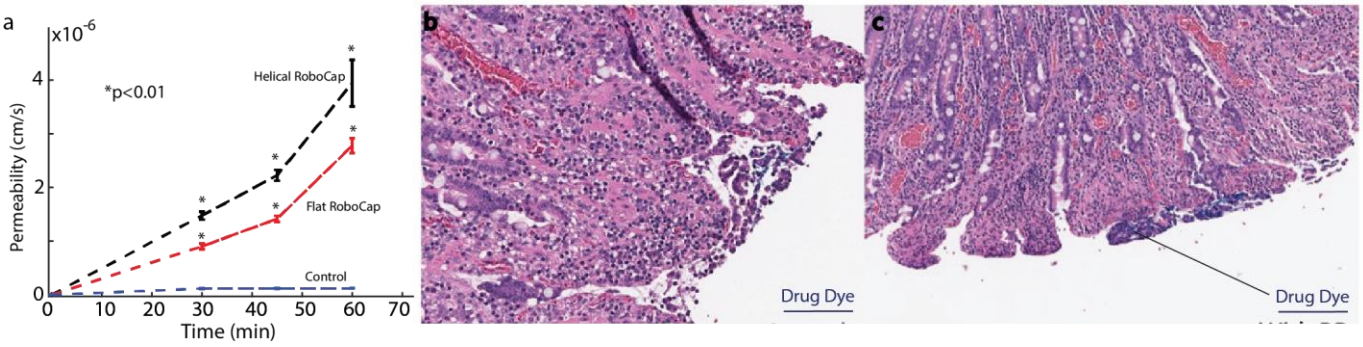

Supplementary Figure 2. a) Permeability of vancomycin in *in vivo* swine small intestine when delivered with the RoboCap and control treatments. The helical and flat RoboCaps demonstrate significantly enhanced uptake ($p < 0.01$, student's two-tailed heteroscedastic t-test). Measurements are from blood sampled from the mesenteric veins. B,C) Hemotoxylin and eosin staining of cross sections of small intestine following treatment with a blue dyed drug to assess permeation in control (b) and treated (c) samples at a magnification of 20x.

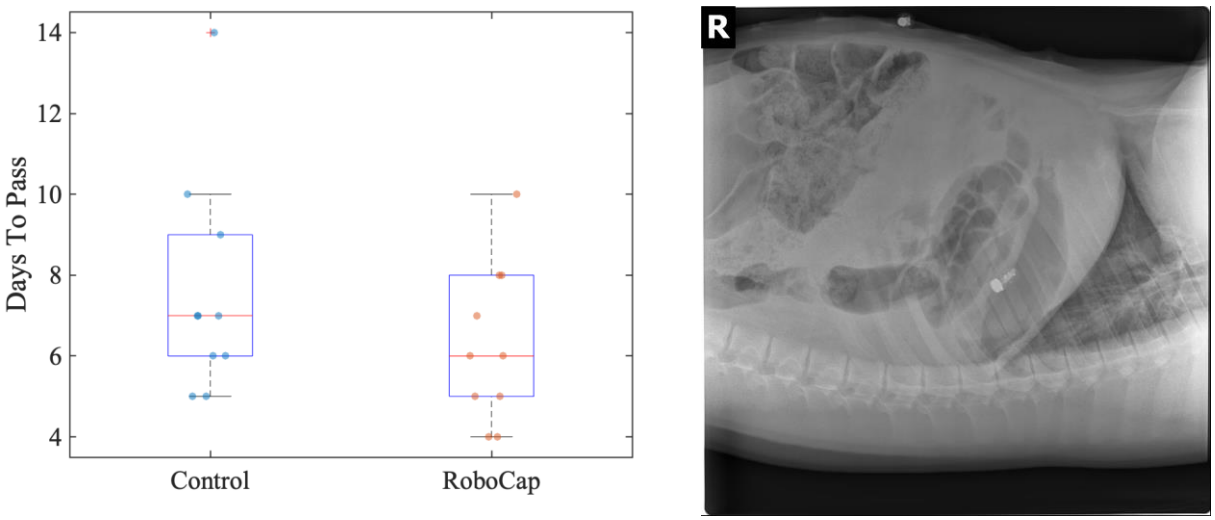

Supplementary Figure 3. Passage Study Left) The time for passage of the radio-opaque beads, a metric of the motility rate, did not significantly change between the control and RoboCap treated animals (n=10/group, p>.1, 2-tailed heteroscedastic t-test). (Right) Representative radiograph of the RoboCap traversing the intestines in a swine.

		Stud Length (um)				
		-Ctrl	**200**	**400**	**800**	**+Ctrl**
FITC MW	**4k**	0.0345	0.036	0.0362	0.0369	0.0402
	40k	0.0354	0.038	0.0381	0.0384	0.0403
	70k	0.0365	0.039	0.0396	0.0399	0.0401
	140k	0.0339	0.038	0.0379	0.0387	0.0405

Average of absorbance values (A.U.) of receiver well contents are quantified from 12 independent samples. Standard error of 5% applied to all readings.

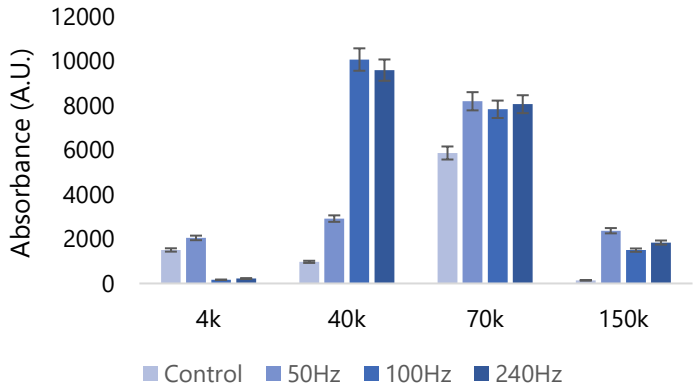

Supplementary Figure 4. Top) Absorbance of receiver well to quantify uptake of FITC-Dextrans of varying molecular weights with RoboCap with studs of varying lengths in a Franz cell diffusion study. In the positive control, mucus was manually removed using a comb-like device brushed against the tissue 10 times at a constant downward force. A negative control in which no mucus was removed and no RoboCap was placed was also utilized. All lengths of studs significantly increased permeability ($p < 0.05$, two-tailed heteroscedastic t-test). Further the permeability increases as the length of the stud increases. Bottom) Uptake of FITC-Dextrans of varying molecular weights with RoboCap operating at 0, 50, 100, or 240 Hz in a Franz cell diffusion study. Means and standard deviations of the absorbance of the receiver well are plotted.

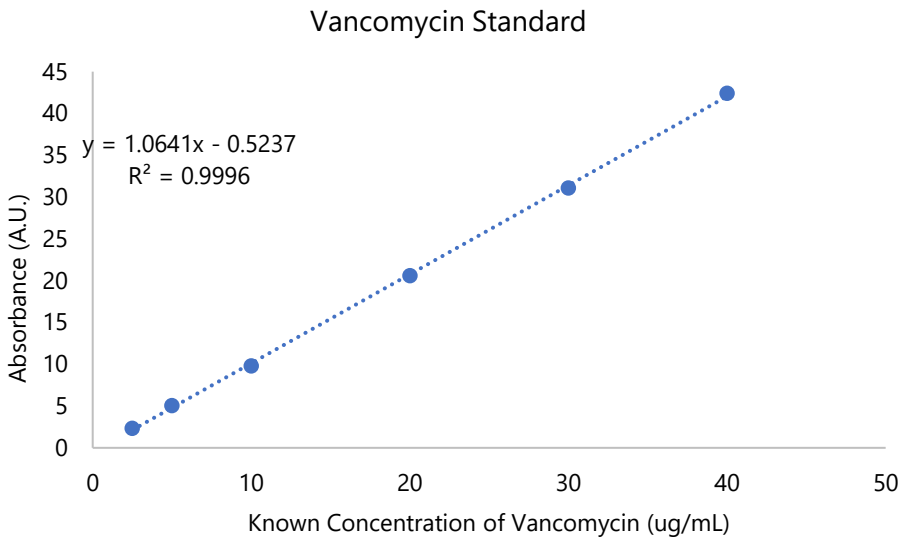

Supplementary Figure 5. Standard curve for vancomycin measurements.

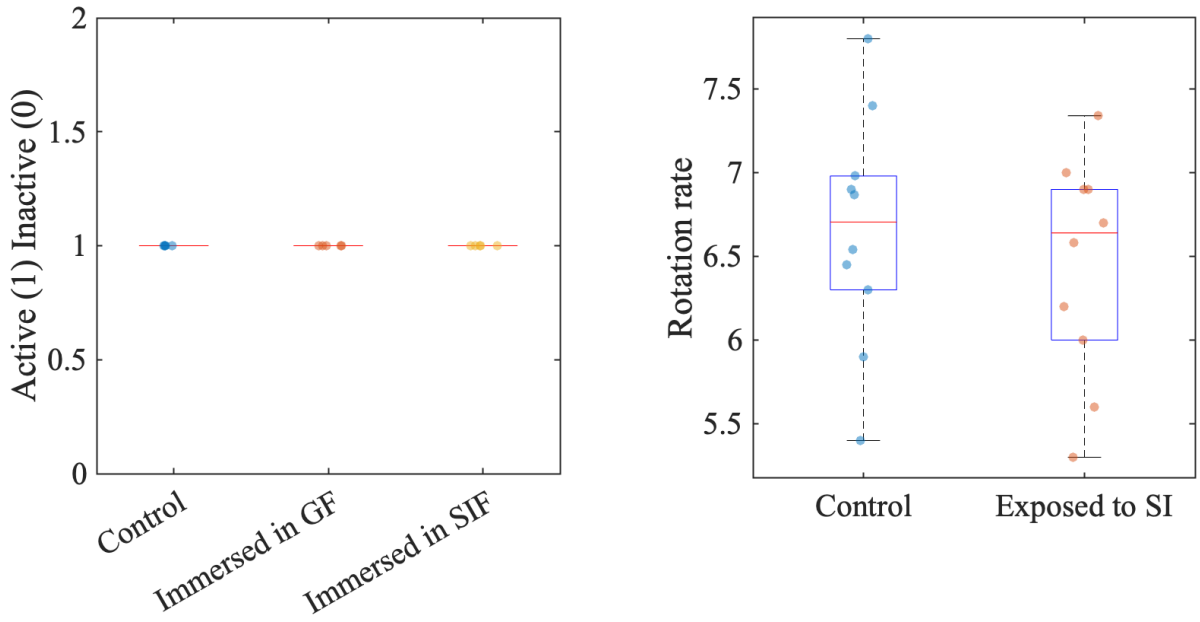

Supplementary Figure 6. Chemical Resistance Test. (Left) RoboCaps exposed to swine gastric fluid (GF), simulated intestinal fluid (SIF) or air (control) for 72 hours at 37°C were tested for activation. All capsules were able to be powered on and function. (Right) Following exposure to small intestinal conditions in swine for at least one hour, the rotation rate of capsules was captured on the benchtop. No significant difference is observed between control and experimental conditions ($p > 0.05$, 2-tailed heteroscedastic t-test).

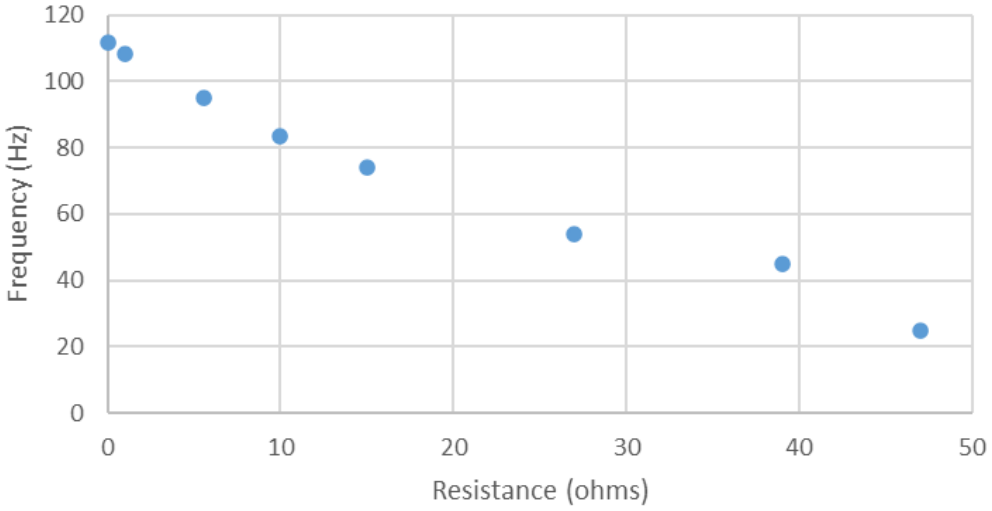

Supplementary Figure 7. The resistor placed in the circuit modulated the operating frequency of the RoboCap. These systems were powered with a 1.55 V, 80mAh silver oxide battery.

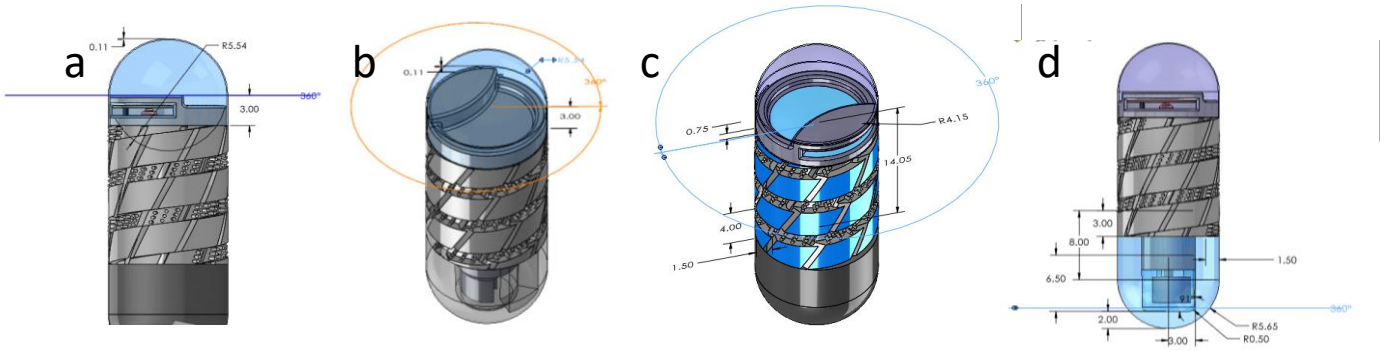

Supplementary Figure 8. Dimensioned schematics of the a) drug cap b) circuit interface c) body and d) motor cap segments of the RoboCap. All units are in millimeters.

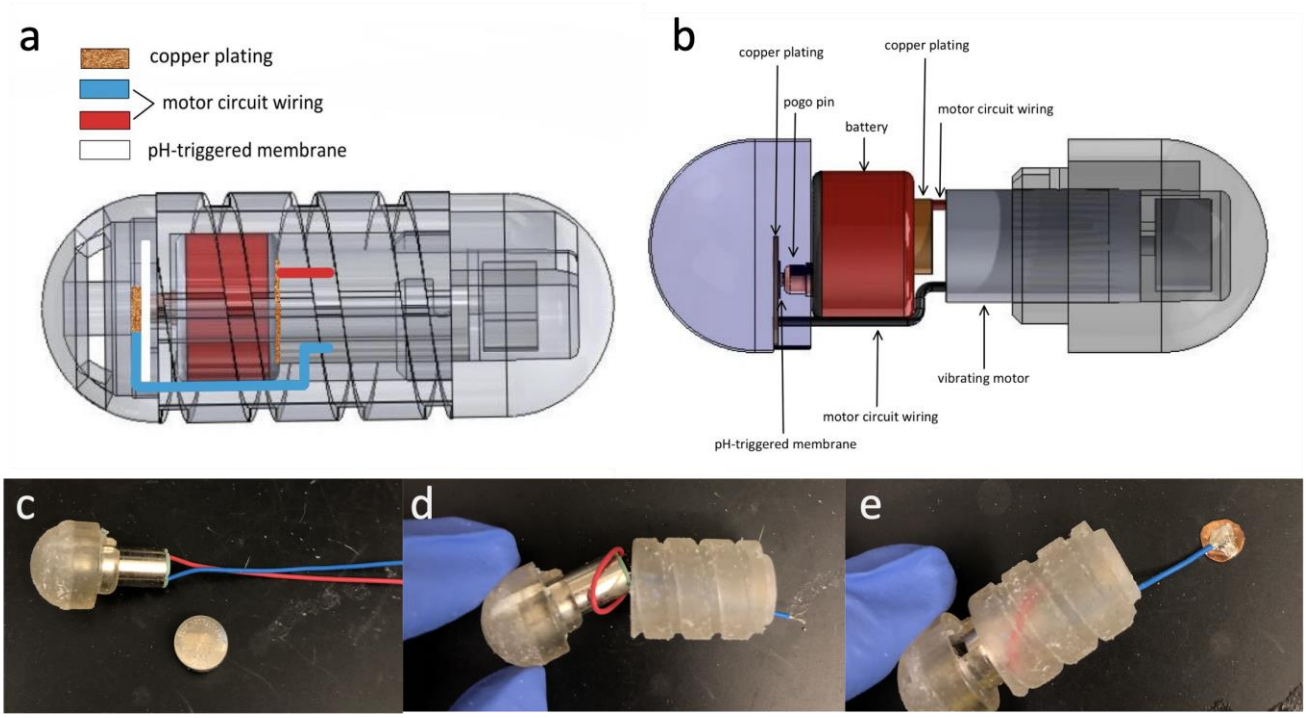

Supplementary Figure 9. Assembly of motor and electrical components of RoboCap. a) Diagram of internal electrical connections and placement of pH-triggered membrane. b) exposed view of internal wiring. c) image of the motor press-into the motor cap d) image of the motor being placed in the body of the RoboCap and e) blue wire being fed through the body of the capsule and soldered to a copper plate.

Supplementary Note 1.

Assembly of RoboCap motor

1. Motor is press fit into motor cap, ensuring the rotating mechanism for vibration of the motor is protected within the motor cap.
2. Copper plating is soldered to the end of both motor wires to enable contacts for circuit completion. Before soldering to the blue wire, the end is fed through the motor body capsule.

Assembly of RoboCap circuit components:

3. Red wire of the vibrating motor is soldered to a copper plate to make contact with the negative battery terminal.
4. The base of the pogo pin is placed in contact with the positive terminal of the battery and completes the RoboCap circuit when touching the copper plate soldered to the blue wire of the motor.
5. Positioned between the pogo pin and copper plate is a pH-triggered membrane preventing the closure of the circuit. The pH triggered membrane is created from Eudragit L, which dissolves at pH $\geq$ 6.
6. Once the RoboCap reaches the small intestine, the dissolution of the pH- triggered membrane results in the completion of the circuit and activation of the motor.

Supplementary Note 2. Detailed analysis of the RoboCap's Motion

The two points along the length of the pill that impart forces affecting the motion are the center of mass, halfway along its length, where the force of gravity acts, and the end of the pill, where the rotating mass imparts forces due to rotational imbalance. The weights rotation result in sinusoidal input forces in the x and z direction, as depicted in Supplementary Figure 10, and rotational momentum in the y direction. The following calculations are neglecting drag due to luminal.

In the x direction, the weight's acceleration relative to the pill will oscillate between the +x and -x direction, while the pill's weight will always be pulling in the -x direction, resulting in an oscillatory behavior of the pill's movement in the x direction moving about a pivot at the other end of the pill. This is what we refer to as the teeter totter effect.

In the z direction, the weight's acceleration relative to the pill will be similar to that of that in the x direction.

In the y direction, there is a conservation of angular momentum, wherein the outer pill rotates in a direction proportional and opposite to the inner offset weight's rotation.

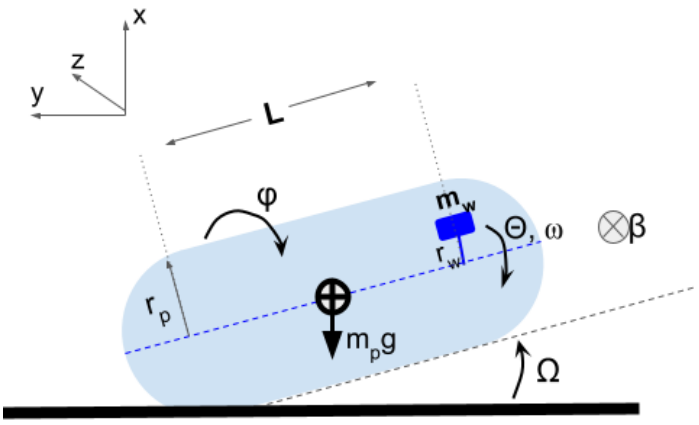

- L: pill length
- Φ: pill rotation angle
- M_w: mass of offset weight
- Θ: offset weight rotation angle
- ω: offset weight constant rotation speed
- r_w: radius of weight offset
- r_p: pill radius
- m_p: total mass of pill
- Ω: angle of pill relative to ground
- g: acceleration due to gravity
- x_w : vertical position of the offset weight
- β : pill angle of rotation about x axis

Supplementary Figure 10. Movement of the RoboCap

Teeter Totter Effect (neglecting drag)

$$x_w = L\Omega + r_p + r_w sin\theta$$
$$\dot{x}_w = L\dot{\Omega} + r_w\dot{\theta}cos\theta$$
$$\ddot{x}_w = L\ddot{\Omega} + r_w\ddot{\theta}cos\theta - r_w\dot{\theta}^2 sin\theta$$
$$\dot{\theta} = \omega\ ;\ \theta = \omega * t$$
$$\ddot{x}_w = L\ddot{\Omega} - r_w\omega^2 \sin(\omega t)$$

Now that we have found the acceleration of the weight relative to the ground, we can balance the moments about the pivot point at the end of the pill.

$$(I_{p/z} - I_{w/z})\ddot{\Omega} = m_p g\frac{L}{2}cos\Omega - m_w\ddot{x}_w L$$
$$(\frac{1}{4}m_p r_p^2 + \frac{1}{3}m_p L^2 - m_w L^2)\ddot{\Omega} = m_p g\frac{L}{2}cos\Omega - m_w L^2\ddot{\Omega} + m_w L r_w\omega^2 \sin(\omega t)$$
$$\ddot{\Omega} = \frac{m_p g\frac{L}{2}}{(\frac{1}{4}m_p r_p^2 + \frac{1}{3}m_p L^2)}cos\Omega + \frac{m_w L r_w\omega^2}{(\frac{1}{4}m_p r_p^2 + \frac{1}{3}m_p L^2)}\sin(\omega t)$$

Matlab ODE45, $\Omega_{initial} = 0$, $\dot{\Omega}_{initial} = 0$

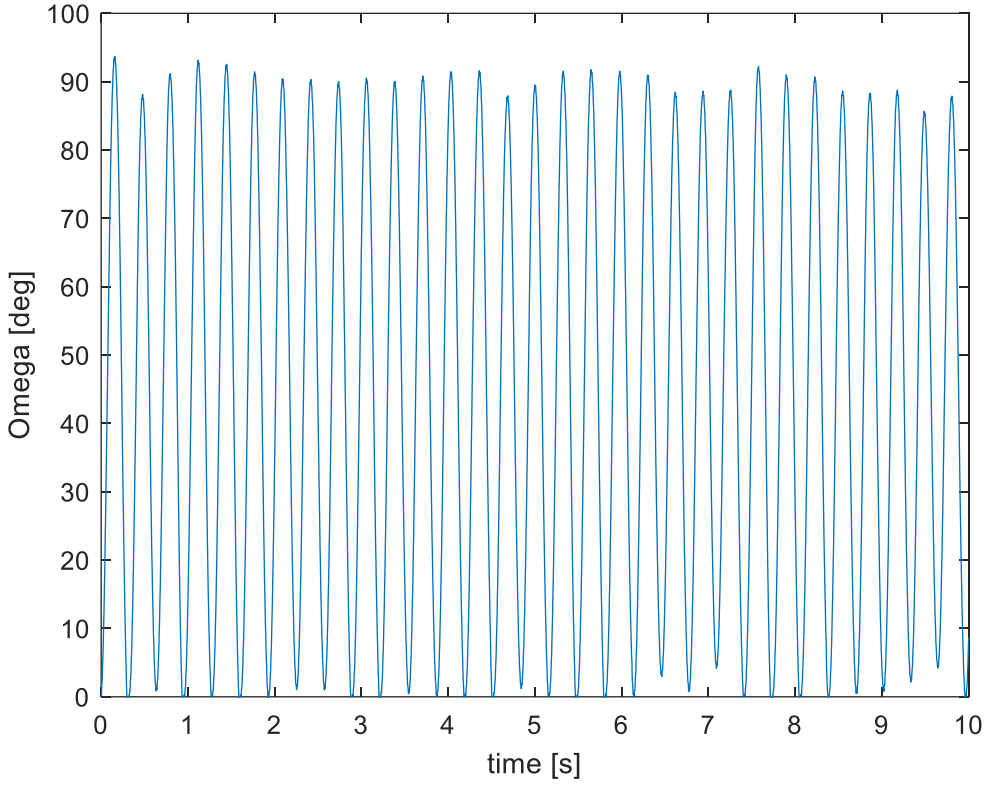

Supplementary Figure 11. Teeter Totter Effect of the RoboCap

Rotation (neglecting drag)

$$I_{p_{/y}}\dot{\varphi} = I_{w_{/y}}\omega$$

$$\dot{\varphi} = \frac{I_{w_{/y}}}{I_{p_{/y}}}\omega = \frac{m_w r_w^2}{m_p r_p^2}\omega \approx .464\,Hz \;\; at \;\; \omega = 100Hz$$

Sideways motion (neglecting drag)

The following is very similar to the process followed for the movement of the pill in the x direction.

$$z_w = L\cos\beta + r_w cos\theta$$

$$\dot{z}_w = -L\dot{\beta}\sin\beta - r_w\dot{\theta}sin\theta$$

$$\ddot{z}_w = -L\dot{\beta}^2\cos\beta - L\ddot{\beta}\sin\beta - r_w\ddot{\theta}sin\theta - r_w\dot{\theta}^2cos\theta$$

$$\dot{\theta} = \omega \; ; \; \theta = \omega * t$$

$$\ddot{z}_w = -L\dot{\beta}^2\cos\beta - L\ddot{\beta}\sin\beta - r_w\omega^2\cos(\omega t)$$

$$(I_{p_{/x}} - I_{w_{/x}})\ddot{\beta} = -m_w\ddot{z}_w L$$

$$(I_{p_{/x}} - I_{w_{/x}})\ddot{\beta} = -m_w L^2\ddot{\beta}sin\beta - m_w L^2\dot{\beta}^2cos\beta - m_w r_w\omega^2 Lcos(\omega t)$$

$$(\tfrac{1}{4}m_p r_p^2 + \tfrac{1}{3}m_p L^2 - m_w L^2)\ddot{\beta} = -m_w L^2\ddot{\beta}sin\beta - m_w L^2\dot{\beta}^2cos\beta - m_w r_w\omega^2 Lcos(\omega t)$$

$$\ddot{\beta} = \frac{-m_w L^2}{(\frac{1}{4}m_p r_p^2 + \frac{1}{3}m_p L^2 - m_w L^2 + m_w L^2 sin\beta)}\dot{\beta}^2 cos\beta - \frac{m_w r_w\omega^2 L}{(\frac{1}{4}m_p r_p^2 + \frac{1}{3}m_p L^2 - m_w L^2 + m_w L^2 sin\beta)}cos(\omega t)$$

Matlab ODE45, $\beta_{initial} = 0$, $\dot{\beta}_{initial} = 0$

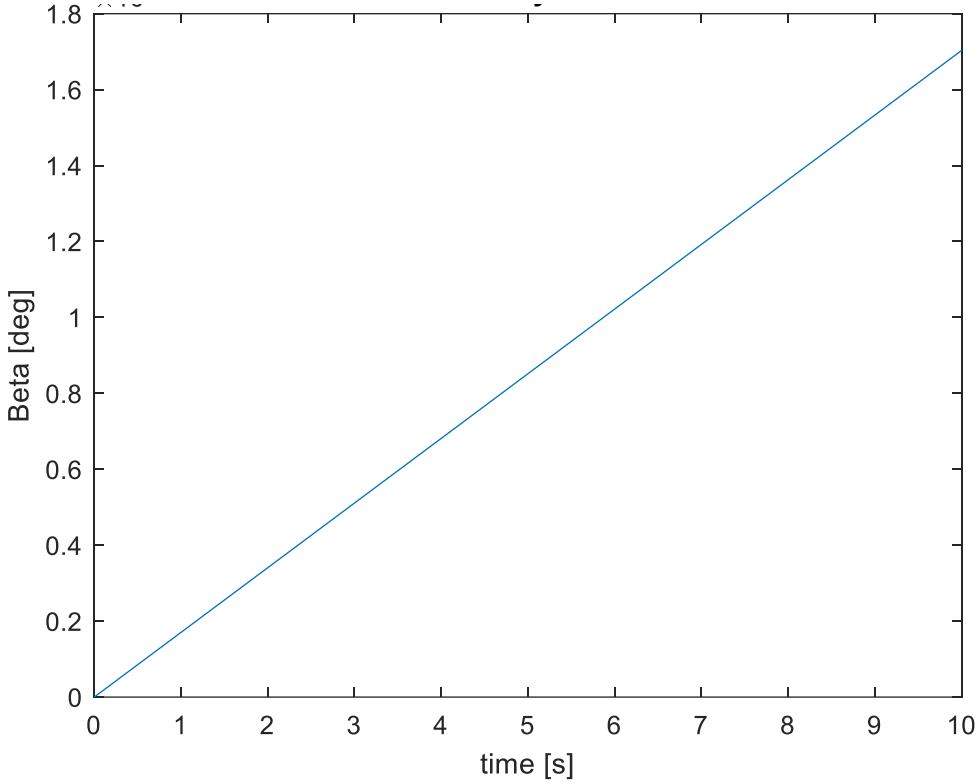

Supplementary Figure 12. Sideways motion of the pill. Degrees are in units of 10^-7.

MATLAB code to perform and visualize the above calculations

```
%% initialize params
clc; clear all;
C_d = .01:.01:1;


r_w = .00125; %radius of weight m
m_w = .00025;%mass of weight kg
m_p = .00425; %mass of pill kg
r_p =  .00445; %radius of pill m
x_w = .0112; %x offset of weight m
l_p = .027; %length of the pill

g = 9.81; %gravity

Iw_y = .5*m_w*(r_w)^2;
Ip_y = .5*m_p*r_p^2;
Ip_x = .25*m_p*r_p^2 + (1/3)*m_p*l_p^2;

f = 100; %frequency Hz
w = f*2*pi;

A = m_p*g*l_p/2;
B = m_w*l_p*r_w*w^2;
C = Ip_x;

AS = Ip_x;
BS = m_w*l_p^2;
CS = m_w*r_w^2*l_p;

%% teeter totter effect
%y(1) is Omega, y(2) is dOmega/dt
% time = 0:.0000001:3;
opts = odeset('RelTol',1e-2,'AbsTol',1e-4,'NonNegative',1);
[t,y] = ode45(@(t,y) vdp1(t,y,A,B,C,w),[0 10],[0; 0],opts);
plot(t,y(:,1).*(180/(2*pi)))
ylabel('Omega [deg]')
xlabel('Time [s]')
title('Pill Teeter-Totter effect')

%% side to side
%y(1) is Beta, y(2) is dBeta/dt
% time = 0:.0000001:3;
% opts = odeset('RelTol',1e-2,'AbsTol',1e-4,'NonNegative',1);
[t,x] = ode45(@(t,x) vdp2(t,y,AS,BS,CS,w),[0 10],[0; 0]);
plot(t,x(:,1).*(180/(2*pi)))
xlabel('Time [s]')
ylabel('Beta [deg]')
title('Pill sideways motion')
%% rotation
dPhi_dt = (1/(2*pi))*Iw_y/Ip_y*w; %Hz


%% ODE function
function dydt = vdp1(t,y,A,B,C,w)
%VDP1  Evaluate the van der Pol ODEs for mu = 1

dydt = [y(2); (A/C)*cos(y(1))+(B/C)*sin(w*t)];
end

function dxdt = vdp2(t,x,AS,BS,CS,w)
```

```
%VDP1  Evaluate the van der Pol ODEs for mu = 1

dxdt = [x(2); (BS/(AS+BS*sin(x(1))))*x(2)*cos(x(1)) - (CS*cos(w*t))/(AS+BS*sin(x(1)))];
end
```

Supplementary Table 1. Histology Scoring

	Edema Score	BM score	Inflammation	Vacuolization	Goblet cells
Control Group	0	1	1	no	PN
	1	1	1	no	PN
	1	0	0	no	PN
	0	0	0	no	PN
	1	2	2	no	PN
	1	2	2	no	PN
	2	2	2	no	PN
	2	2	2	no	PN
	1	2	2	no	PN
Average	**1**	**1.33**	**1.33**		
Standard Deviation	**0.70**	**0.86**	**0.86**		
Experimental Group	0	1	1	yes	PN
	1	1	2	yes	PN
	1	1	2	yes	PN
	1	1	2	yes	PN
	1	0	1	no	PN
	1	0	1	no	PN
	1	0	1	yes	PN
	1	0	1	yes	PN
	1	1	1	no	PN
	1	1	1	no	PN
	1	1	1	no	PN
	1	1	1	no	PN
	1	1	1	no	PN
	1	1	2	no	PN
	1	1	2	no	PN
	1	1	1	no	PN
Average	**0.93**	**0.75**	**1.31**		
Standard Deviation	**0.25**	**0.44**	**0.47**		
Scale	0 - absent 1- mild 2 - moderate 3 - marked	0 - intact 1- partially disrupted 2 - multifocal disruption	0 - absent 1- focal acute inflammation 2 - multifocal acute inflammation		PN present/normal in number and configuration

Supplementary Table 2. Assessment of Small Intestinal Epithelium demonstrates no significant differences between experimental and control groups.

Group	Stain	Epithelium	Surface brush border	intraepithelial lymphocytes per 50 enterocytes	Surface lamina propria	Final epithelial assessment
Control	H&E	0	0	3.00	0	No histopathological abnormalities
	H&E	0	0	2.00	0	No histopathological abnormalities
	H&E	1	0	2.00	0	No histopathological abnormalities
	H&E	0	0	1.00	0	No histopathological abnormalities
	H&E	2	0	2.00	0	No histopathological abnormalities
	H&E	0	0	8.00	0	No histopathological abnormalities
	H&E	0	0	2.00	0	No histopathological abnormalities
	H&E	0	0	2.00	1	No histopathological abnormalities
	H&E	0	0	1.00	0	No histopathological abnormalities
	H&E	0	0	1.00	0	No histopathological abnormalities
	Trichrome	0	0	1.00	0	No histopathological abnormalities
	Trichrome	0	0	1.00	0	No histopathological abnormalities
	Trichrome	0	0	1.00	0	No histopathological abnormalities
Average				**2.17**		
Standard Deviation				**1.95**		
Experimental Group	H&E	0	0	1.00	1	No histopathological abnormalities
	H&E	0	0	2.00	0	No histopathological abnormalities
	H&E	0	0	1.00	0	No histopathological abnormalities

	H&E	0	0	2.00	0	No histopathological abnormalities
	H&E	1	0	1.00	0	No histopathological abnormalities
	H&E	1	0	7.00	0	No histopathological abnormalities
	H&E	0	0	2.00	0	No histopathological abnormalities
	H&E	0	0	4.00	0	No histopathological abnormalities
	H&E	0	0	2.00	0	No histopathological abnormalities
	H&E	0	0	7.00	1	No histopathological abnormalities
	Trichrome	2	0	2.00	0	No histopathological abnormalities
	Trichrome	2	0	1.00	0	No histopathological abnormalities
	Trichrome	0	0	1.00	0	No histopathological abnormalities
Average		**0.46**	**0.00**	**2.54**	**0.15**	
Standard Deviation		**0.78**	**0.00**	**2.15**	**0.38**	
P-value of 2 tailed heteroscedastic t-test		0.40	1.00	0.57	0.56	
Scale		0 - Surface Epithelium Intact 1 - Mild surface attenuation 2 - focal surface attenuation	0 - intact 2 - disintegrated		0 - no alteration 1 - slightly increased inflammation 2- moderate inflammation 3 - severe inflammation	